Biomaterials 203 (2019) 31–42

Contents lists available at ScienceDirect

Biomaterials

journal homepage: www.elsevier.com/locate/biomaterials

Cellulose nanocrystals modulate alveolar macrophage phenotype and phagocytic function

Johanna Samulin Erdem[a,*], Mayes Alswady-Hoff[a,1], Torunn K. Ervik[a,1], Øivind Skare[a], Dag G. Ellingsen[a], Shanbeh Zienolddiny[a]

[a] National Institute of Occupational Health, Oslo, Norway

ARTICLE INFO

Keywords:
Macrophage polarization
Phagocytosis
Nanocellulose
Cytotoxicity
Pro-inflammatory signaling
Acute inflammation

ABSTRACT

Nanocellulose is a promising bio-nanomaterial with attractive properties suitable for multiple industrial applications. The increased use of nanocellulose may lead to occupational exposure and negative health outcomes. However, knowledge on its health effects is limited, and while nanocellulose exposure may induce acute inflammatory responses in the lung, the underlying mechanisms are unknown. Alveolar macrophages are key cells in alveolar particle clearance. Their activation and function may be affected by various particles. Here, we investigated the uptake of pristine cellulose nanocrystals (CNC), and their effects on alveolar macrophage polarization and biological function. CNC uptake enhanced the secretion of several cytokines but did not on its own induce a complete macrophage polarization. In presence of macrophage activators, such as LPS/IFNG and IL4/IL13, CNC exposure enhanced the expression of M1 phenotype markers and the secretion of pro-inflammatory cytokines and chemokines, while decreasing M2 markers. CNC exposure also affected the function of activated alveolar macrophages resulting in a prominent cytokine burst and altered phagocytic activity. In conclusion, CNC exposure may result in dysregulation of macrophage activation and function that are critical in inflammatory responses in the lung.

1. Introduction

Nanocellulose (NC) is a promising bio-nanomaterial with attractive properties suitable for multiple industrial applications in material science and biomedical engineering. Due to their renewable nature, low production costs, mechanical properties, biocompatibility, and optical properties, NC has potential in many fields, such as nanocomposite materials, surface and rheology modifiers, films and foams, specialty papers, food additives, and biomedical devices. NC materials are of particular interest in various Norwegian and European industries, and high scale production of NCs and growing number of applications have led to increased focus on their health effects and safety [1]. NC can be obtained from a variety of sources, including trees/plants, algae and bacteria, gaining materials of diverse dimensions and surface characteristics. Cellulose nanocrystals (CNC) are produced by acid hydrolysis, whereas, mechanical processing often together with chemical pretreatment yields cellulose nanofibers (CNF) [2]. The different types of NCs exhibit distinct properties affecting their applicability and functionality in different applications. Moreover, the surface of the NCs can be modified by addition of functional groups to impart specific functionality.

While data on health effects in workers exposed to NC are largely unavailable [3], high aspect ratios and biodurability of NC in human lung [4] are of concern, and makes it important to investigate the toxicological properties of NC materials. Toxicological testing of NC materials has proven challenging, as different raw materials, preparation procedures, and post-processing techniques yield a wide range of NCs with varied physicochemical properties. The scarce toxicological data available could indicate that NC materials induce only low or moderate cytotoxic and genotoxic effects *in vitro* and *in vivo* [5–7]. However, several studies have demonstrated that NC induces acute pulmonary inflammation in mice following inhalation [8–10]. Mice exposed to CNC through pharyngeal aspiration had a pronounced acute dose-dependent inflammatory response at 24 h of exposure and after repeated exposures [9,10]. Furthermore, animals exposed to CNF show increased recruitment of inflammatory cells in the lungs, and accumulation of particles in the bronchi, the alveoli and in the cytoplasm of pulmonary macrophages [8]. On contrary, long term effects of CNC on

* Corresponding author. Department of Biological and Chemical Work Environment, National Institute of Occupational Health, N-0033, Oslo, Norway.
E-mail address: Johanna.Samulin-Erdem@stami.no (J. Samulin Erdem).
[1] These authors contributed equally.

https://doi.org/10.1016/j.biomaterials.2019.02.025
Received 26 November 2018; Received in revised form 22 February 2019; Accepted 28 February 2019
Available online 28 February 2019

pulmonary inflammation have not been observed and a gradual time-dependent alleviation of inflammation response was suggested in a recent study by Park et al. [11]. Similarly, CNC exposure causes inflammatory responses and elevated levels of inflammatory cytokines in pulmonary epithelial cells, monocyte cultures, and in 3D co-cultures of epithelial, monocyte and dendritic cells [12–14]. Interestingly, functionalization may affect the inflammatory potential of NCs as carboxymethylation and carboxylation lower the inflammatory potential of NC materials [15,16].

To date, the underlying mechanisms for the observed induction in pulmonary inflammation following NC exposure have not been addressed. Inflammatory signaling is important in the development of chronic pulmonary diseases such as asthma and chronic obstructive pulmonary disease (COPD). Resident alveolar macrophages hold key roles in development of these conditions as they are the main cell type involved in pathogenic clearance in the lung and important players in pulmonary inflammation. The diverse biological activities of macrophages are mediated by phenotypically distinct subpopulations generated through a process called macrophage polarization [17]. Macrophage polarization is a dynamic process, where M1 and M2 macrophages represent two extremes of activation. Macrophage activation by lipopolysaccharide (LPS), interferon gamma (IFNG) and tumor necrosis factor alpha (TNFA) results in a M1 macrophage phenotype, whereas, interleukin 4 (IL4), IL13 and IL10 stimulation induces M2 polarization. M1 macrophages are predominately responsible for the clearance of intracellular pathogens by releasing pro-inflammatory cytokines and promoting a local Th1 environment during initiation of inflammation. M2 macrophages have more diverse phenotypes characterized by their involvement in Th2 responses. The respective roles of M1 and M2 macrophages in respiratory diseases are complex and fine-tuning of macrophage polarization is vital as imbalance may have detrimental effects resulting in states of inflammation and disease. Besides classical macrophage activators, different particles including nanoparticles may perturb the polarization and reprogramming of macrophages and affect their immunological functions. The physiochemical properties of particles such as chemical composition, size and surface coatings determine the effects on macrophage polarization [18]. Studies show that several types of nanoparticles including gold, silver, zinc oxide, silica, titanium dioxide and multi-walled carbon nanotubes may induce a pro-inflammatory M1 phenotype, however, there are discrepancies between the different studies illustrating the difficulties in generalizing the effects of nanoparticles, reviewed by Miao et al. [18]. Moreover, phagocytized CNC particles are not degraded in the macrophage phagolysosome as the acidic pH is insufficient to degrade cellulose [4]. Hence, in the alveoli, CNC materials are likely cleared by mechanical movement of macrophages out of the alveoli, a process that can take months to years [4]. Prolonged retention of CNC particles within resident alveolar macrophages could also affect macrophage functions such as the ability to engulf foreign materials, present antigens and cytokines.

The main aim of this study was to investigate if macrophage polarization is a contributing mechanism to the acute inflammation observed in animals following pulmonary NC exposure. Increased mechanistic understanding of macrophage-particle interactions may give valuable insight into the development of exposure-related pulmonary diseases. In light of the anticipated role of M1 macrophages in local pre-inflammatory Th1 responses [12,14] and evidence of pronounced acute inflammatory responses in CNC-exposed lungs [9,10], we postulated that CNCs promote alveolar macrophage polarization in exposed lungs to regulate the initiation and resolution of acute pulmonary inflammation. To address this, we investigated phenotypic and functional changes in alveolar MH-S macrophage cells following exposure to two pristine, well characterized CNC materials.

2. Materials and methods

2.1. Particle preparation and characterization

Freeze dried CNC powder (CNC_{dry}) and 12.1% CNC gel (CNC_{gel}) were obtained from the University of Maine Process Development Centre (Orono, ME) and were manufactured from wood pulp at the US Forest Service's Cellulose Nanomaterials Pilot Plant (Forest Products Laboratory (FPL), Madison, WI). CNCs are rod-like particles with dimensions of approximately 5 nm in diameter and 150–200 nm in length. The particles were sterilized by autoclaving and endotoxin levels were assessed by kinetic chromogenic limulus amebocyte lysate (LAL) assay according to the manufacturer's instructions (Lonza, Basel, Switzerland). Endotoxin levels for the particles were below the detection limit of 0.005 EU/ml. Stock dispersions were prepared in sterile ultrapure water at a concentration of 3 mg/ml and vortexed for 30 s to ensure even dispersion. Zeta potential and hydrodynamic diameter measurements by dynamic light scattering (DLS) were conducted on stock solution and CNC dispersions in media (ZetaSizer Nano ZS, Malvern Instruments Ltd, Malvern, UK). 1.59 was used as refractive index. Scanning electron microscope (SEM) samples were prepared as previously described by Kunaver et al. [19]. In brief, CNC samples were dispersed at a concentration of 18 μg/ml in acetone, sonicated 15 min and 20 μl was placed on a pre-warmed glass slide and allowed to dry. The specimens were sputter-coated with 2.4 nm platinum in a Cressington 208HR (Cressington Scientific Instruments, Watford, England) sputter coater and analyzed with a Hitachi SU 6600 (Hitachi High-Technologies Corporation, Tokyo, Japan) field emission scanning electron microscope (FE-SEM). The instrument was operated under the following conditions: accelerating voltage of 20 kV and working distance of 10 mm. High resolution images of the particles were obtained by acquiring at slow scanning speed.

2.2. Cell culture and particle exposure

Murine alveolar macrophages, MH-S (CRL-2019, ATCC, Rockville, MD) were maintained in ATCC-formulated RPMI-1640 medium (Gibco, ThermoFisher Scientific, Waltham, MA) supplemented with 10% FBS (Gibco, ThermoFisher Scientific), and 50 μM β-mercaptoethanol (Gibco, ThermoFisher Scientific) in 5% CO_2 at 37 °C. Cells were polarized towards M1 phenotype with LPS (1 ng/ml, Sigma Aldrich, St Louis, MO) and/or IFNG (20 ng/ml, PeproTech, Rocky Hill, NJ), or to M2 phenotype with IL4 (20 ng/ml, PeproTech) and IL13 (20 ng/ml, PeproTech) for up to 48 h. Macrophage subsets were characterized by differential gene expression of a selected panel of cell surface molecules, cytokines/chemokines and regulatory proteins. The restricted panel was selected based on literature reports and on their involvement in murine macrophage activation [20–22]. Accordingly, LPS/IFNG treatment (M1 polarization) resulted in increased expression of c-x-c motif chemokine ligand 9 (*Cxcl9*, also known as *Mig*), and nitric oxide synthase 2 (*Nos2*) after 24 h of polarization and increased expression of *Cxcl9, Il1b, Il6, Nos2* after 48 h of polarization, Supplementary Figure S1. Moreover, an increase in the secretion of IL1B (9.90 vs 12.82 pg/ml), IL6 (1.00 vs 13.81 pg/ml) and CXCL9 (undetected vs 3800 pg/ml) was observed when comparing M0 and M1 cells (controls) in Supplementary Tables S1 and S2. Treatment with IL4/IL13 (M2 polarization) induced the expression of arginase 1 (*Arg1*), cytokine inducible SH2 containing protein (*Cish*), eosinophil-associated ribonuclease A family member 11 (*Ear11*) and mannose receptor C-type 1 (*Mrc1*, previously known as *Cd206*), Supplementary Figure S1. MH-S cells were exposed to CNC particles to evaluate their ability to induce macrophage polarization. Moreover, cells were exposed to CNCs in presence of inducers of polarization to evaluate potential interference with the polarization process or 24 h after polarization initiation to evaluate effects on polarized cell functions.

2.3. Analysis of cellular uptake of CNC materials and investigation of uptake mechanisms

Cells were seeded at concentrations of 2.5 E^5 cells/well (6.6 E^4 cell/cm^2) for M0 and M2 polarized cells and 3.5 E^5 cells/well (9.2 E^4 cell/cm^2) for M1 polarized cells on coverslips in 12-well plates. After cell attachment the cells were polarized for 24 h. For quantification of cellular uptake, the cells were exposed to 5 μg/cm^2. After optimization, cellular uptake was assessed at 2 h, 6 h and 24 h post-exposure. For assessment of uptake mechanisms, cells were pretreated with latrunculin B (2.5 μM, 30 min, Sigma Aldrich) or wortmannin (300 nM, 15 min, Acros Organics, ThermoFisher Scientific). Inhibitor doses were optimized, and TMR-conjugated 70 kDa dextran (125 μg/ml, 15 min, ThermoFisher Scientific) or pHrodo Ecoli (150 μg/ml, 2 h, Invitrogen, ThermoFisher Scientific) were used as positive controls. After pretreatment, the cells were exposed to CNC particles for 2 h or 6 h. Visualization of CNC particles were performed using a biotinylated carbohydrate binding module (CBM) of β-1,4-glycanase (EXG:CBM) essentially as previously described [12,23], with minor modifications. EXG:CBM protein was a kind gift from Dr H. Wolff (Finnish Institute of Occupational Health, Finland) and Prof. U. Vogel (National Research Centre for Work Environment, Denmark). In brief, the cells were fixed in ice-cold acetone for 10 min and blocked by incubation with 30% rabbit serum (AgriSera, Vännäs, Sweden) in PBS for 10 min at room temperature. Endogenous biotin was blocked by Streptavidin/Biotin Blocking Kit according to the manufacturer's instructions (Vector Laboratories, Burlingame, CA). CNC materials were stained using biotinylated EXG:CBM protein at 1:300 dilution in 2% rabbit serum-PBS for 60 min at room temperature. EXG:CBM protein was visualized by Streptavidin Alexa Fluor 488 conjugate, according to the manufacturer's recommendations (Invitrogen, ThermoFisher Scientific). Cells were counterstained with Alexa Flour 647 Phalloidin (Invitrogen, ThermoFisher Scientific) to stain F-actin and mounted with ProLong Gold antifade reagent with DAPI (Invitrogen, ThermoFisher Scientific). Fluorescent staining was visualized using a pinhole laser confocal microscope (Zeiss, Oberkochen, Germany) and images were acquired using an AxioCam camera (Zeiss). Cellular uptake was quantified from the acquired images using ImageJ. To visualize cellular uptake of the doses used in the study (1.5, 15 and 45 μg/cm^2) cells were exposed for 24 h.

2.4. Cell viability and proliferation assays

For assessment of cell viability the cells were seeded at a concentration of 1.6 E^5 cell/well (4.6 E^4 cells/cm^2) in 12-well plates and allowed to attach overnight. The following day the cells were polarized and 24 h after polarization the cells were exposed to CNC particles (0, 1.5, 5, 15, 45 and 90 μg/cm^2). Cells were incubated with particles for 24 h and cell viability was assessed by Pierce™ lactate dehydrogenase (LDH) Cytotoxicity Assay Kit (ThermoFisher Scientific) and by flow cytometry using ReadiDrop Cell Viability Assay (Bio-Rad Laboratories Ltd, Hercules, CA) according to the manufacturers' instructions. Shortly, cell medium was collected and extracellular LDH levels were assessed by absorbance measurements at 490 nm and 680 nm using the SpectraMax i3 (Molecular Devices, San Jose, CA). Cells were harvested and counted using trypan blue to assess cell proliferation. The cells were washed in PBS, filtered through a 100 μm cell strainer and cell concentrations were adjusted to 2.0E^6 cells/ml. Cells were stained with ReadiDrop Propidium Iodide (PI) and analyzed on a CytoFLEX flow cytometer using the CytExpert software (Beckman Coulter, Brea, CA). Data were collected for 10,000 live events per sample. Doublets were excluded prior to analysis.

2.5. Gene expression analysis

For analysis of gene expression patterns, cells were seeded at a concentration of 6.0 E^5 cell/well (1.7 E^5 cells/cm^2) in 12-well plates. The following day the cells were exposed to CNC particles at the concentrations 0, 1.5, 15, 45 μg/cm^2 with/without polarization inducers or cells were polarized for 24 h and thereafter exposed to CNC particles for an additional 24 h. Total RNA was isolated using the Total RNA Purification Plus Kit according to the manufacturer's instructions (Norgen Biotek Corp., Ontario, Canada). Total RNA was reverse transcribed using qScript cDNA synthesis kit (Quanta BioSciences, Beverly, MA), following the manufacturer's instructions. Gene expression was analyzed by qPCR using SYBR Green I technology on the QuantStudio 5 Real-Time PCR System (Applied Biosystems, ThermoFisher Scientific). Primer sequences (KiCqStart™ Primers, Sigma Aldrich) are available upon request. Expression was normalized to the geometric mean of ubiquitin C (*Ubc*) and beta-2-microglobulin (*B2m*), which were used as housekeeping genes. Relative expression was assessed using relative standard curve approach. Cq values ≥ 34 were set as non-detectable.

2.6. Analysis of cytokine and chemokine secretion

Concentrations of 24 mouse cytokines/chemokines in culture media were measured by Bio-Plex Pro™ Mouse Cytokine 23-plex and CXCL9 single-plex assays (Bio-Rad Laboratories Ltd) according to manufacturer's instructions on a Luminex MAGPIX® System using the xPONENT Software (Luminex Corp., Austin, TX). Concentrations were normalized to correct for variations in cell numbers. Proteins used for polarization were excluded for the analysis of the respective cell lines, *i.e.* INFG in M1 cells and IL4 and IL13 in M2 cells. C-c motif chemokine ligand 3 (CCL3, previously known as MIP1A) was excluded as high basal secretion levels made the samples impossible to quantify as they were outside the range of the standard curve. Heat map and hierarchical clustering analysis with Euclidean distance were performed using the ComplexHeatmap package version 1.12.0 in R version 3.4.3.

2.7. Phagocytosis

For analysis of phagocytosis, macrophages were seeded at a concentration of 7500 cells/well (2.3 E^4 cells/cm^2) in a 96-well plate. The cells were polarized for 24 h and exposed to CNC materials for an additional 24 h. Effects of CNC materials on macrophage phagocytic capacity were assessed using the IncuCyte pHrodo Ecoli as described by the manufacturer (Essen BioScience, Ann Arbor MI). For live-cell imaging of macrophage phagocytosis, the cells were incubated with bioparticles in FluoroBrite™ DMEM (Gibco, ThermoFisher Scientific) and images were taken every 15 min for 12 h using the IncuCyte Zoom live cell imaging system (Essen BioScience). Phagocytosis was assessed by the IncuCyte Zoom software using Top-Hat background subtraction and visualized as phagocytosis intensity (μm^2/image). This metrics visualized both the number of active phagosomes and their maturity. The data was normalized to correct for variations in cell numbers. Differences between treatments were assessed by linear regression analysis of the exponential increase phase of the phagocytic intensity curve.

2.8. Statistical analysis

Gene expression and cytokine/chemokine secretion data were analyzed by linear mixed effects models using the lmer function in the lme4 package for R (version 3.4.3). p-values were adjusted with the Benjamini & Hochberg (BH) step-up FDR-controlling procedure. p-values < 0.05 were considered significant.

3. Results

3.1. Characterization of CNC materials

Representative SEM images of CNC materials are shown in Fig. 1A.

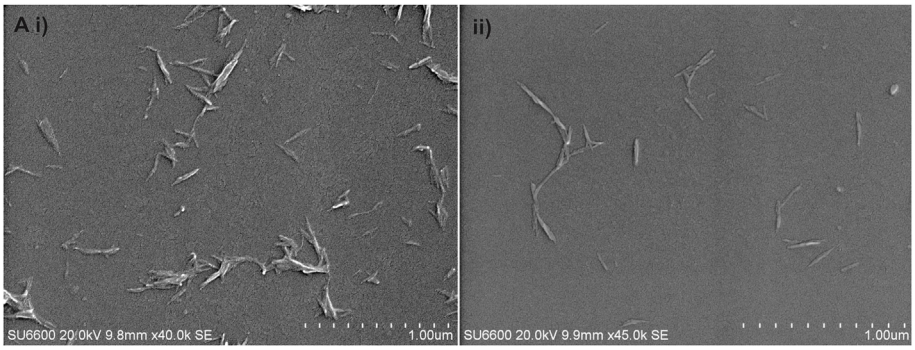

Fig. 1. Characterization of CNC particles. (A) Representative SEM images of (i) CNC_{dry} and (ii) CNC_{gel} particles. (B) Hydrodynamic diameter and zeta potential measurements were conducted in (i) water and (ii) cell culture media. Abbreviations: Z-Ave, Z-average; d.nm, diameter in nm; PdI, polydispersity index; ZP, zeta potential; SD, standard deviation.

B i)

Nanoparticle	Z-Ave (d.nm)	PdI	ZP (mV)	SD
CNC_{dry}	153.0 ± 5.8	0.41 ± 0.06	-47.0	0.95
CNC_{gel}	135.9 ± 2.5	0.25 ± 0.01	-48.1	1.25

ii)

Nanoparticle	Z-Ave (d.nm)	PdI	ZP (mV)	SD
CNC_{dry}	1133.7 ± 65.1	0.95 ± 0.03	-14.2	0.36
CNC_{gel}	774.9 ± 4.3	0.98 ± 0.02	-13.5	0.15

Measurement of individual particles confirmed average lengths of 159.8 ± 45.2 and 155.0 ± 40.8 nm and average widths of 21.8 ± 4.7 and 19.8 ± 4.1 nm for CNC_{dry} and CNC_{gel}, respectively. Average aspect ratios were calculated to be 7.3 for CNC_{dry} and 7.8 for CNC_{gel}. DLS analysis showed average hydrodynamic diameters (Z-Ave) of 153.0 ± 5.8 and 135.9 ± 2.5 nm for CNC_{dry} and CNC_{gel}, respectively, in water. DLS analysis of CNC particles in media showed increased hydrodynamic diameters and high polydispersity indexes of the particles compared with particles in water indicating a broad size distribution and an increased occurrence of aggregation/agglomeration of the particles in the media. This is supported by data from zeta potential measurements indicating that the particles have a higher degree of stability in water than in media, and are more likely to form agglomerates/aggregates in the media, Fig. 1B.

3.2. Cellular uptake of CNC materials in unpolarized and polarized macrophages

Quantification of cellular uptake was assessed by immunofluorescence and presented as the percentage of cells that had visible phagocytic vacuoles present in the cytoplasm (% CNC + cells), Fig. 2. Regardless of polarization, CNC_{gel} particles were more efficiently taken up than CNC_{dry} particles. Cells exposed to CNC_{dry} particles had more agglomerates present at the cell surface, Fig. 2A(ii). Moreover, the kinetics of cellular uptake was different between the various polarization phenotypes. While, 48% of M1 and 36% of M0 macrophages had internalized CNC_{gel} particles at 2 h of exposure, only 14% of M2 cells had taken up CNC_{gel} particles at this time point. At 24 h of exposure the differences were no longer present and the cells showed a high uptake of CNC_{gel} regardless of macrophage activation, Fig. 2B. Moreover, M1 macrophages had a generally low uptake of CNC_{dry} compared to M0 and M2 macrophages, Fig. 2A. Visualization of doses used for cellular exposure at 24 h are to be found in Supplementary Figure S2, and especially the high dose 45 μg/cm^2 CNC_{dry} resulted in agglomerates at the cell surface possibly indicating an overload of particle clearance at high exposure levels, as exemplified in M2 polarized cells in Supplementary Figure S3.

3.3. Mechanism of cellular uptake of CNC materials

There are several potential pathways that can be involved in cellular uptake of nanomaterials. However, macrophages internalize pathogens and foreign material primarily through phagocytosis and macropinocytosis. To investigate, whether, these mechanisms are involved in the internalization of CNC materials, the F-actin inhibitor, latrunculin B, and the phosphoinositide 3-kinase (PI3K) inhibitor, wortmannin, were used, Fig. 3. Effects of these agents were assessed following CNC_{gel} exposure for 2 h. Since the cells had a very low uptake of CNC_{dry} particles at 2 h, effects of inhibitors were investigated following 6 h of CNC_{dry} exposure. The percentage of cells that showed visible vacuoles following CNC_{gel} exposure was significantly reduced by latrunculin B and wortmannin treatment, Fig. 3B. This was also observed for CNC_{dry} particles in M2 cells, Fig. 3A. While a similar response was observed for M0 and M1 cells exposed to CNC_{dry}, the data are more uncertain as the percentage of cells with internalized CNC_{dry} was very low. These data indicate that phagocytosis/macropinocytosis are possibly the main mechanisms of CNC uptake in MH-S macrophages.

3.4. Effects of CNC materials on macrophage viability and proliferation

For analysis of viability and proliferation macrophages were exposed to various concentrations of CNC materials. CNC exposure at low concentrations (1.5 and 5 μg/cm^2) did not induce significant cytotoxicity as analyzed by incorporation of DNA label and LDH assay. However, at higher doses, CNC_{dry} exposure induced a slight decrease in cell viability assessed by incorporation of DNA label. Moreover, exposure to both CNC materials did not affect cell proliferation significantly, and only in M1 cells exposed to CNC_{gel} at the highest dose (90 μg/cm^2) a small reduction in cell number was observed, Supplementary Figure S4.

3.5. Effects of CNC exposure on macrophage polarization

CNC exposure alone was not sufficient in inducing a full polarization phenotype of murine alveolar macrophages as no changes in M1 or M2 gene expression markers of polarization were observed (data not shown). Unpolarized M0 macrophages had a generally low secretion of cytokines and chemokines. However, CNC exposure led to increased secretion of IFNG, IL3, IL4 and IL12P40, and of colony stimulating factor 3 (CSF3, previously known as G-CSF), CCL2 (also known as MCP1) and CCL11 (previously known as eotaxin), Fig. 4, Supplementary Table S1.

Whilst CNC exposure alone did not induce a complete polarization, CNC exposure in presence of other inducers of macrophage polarization (*i.e.* IFNG and IL4/IL13) on contrary promoted a more prominent M1 phenotype and a pro-inflammatory response compared with unexposed control cells (stimulated with IFNG or IL4/IL13). Exposure of macrophages with CNC_{dry} or CNC_{gel} in presence of IFNG resulted in increased expression of *Il1b*, whereas exposure with CNC_{gel} also increased the expression of M1 markers *Cxcl9*, *Il6*, *Nos2* and *Tnfa*, as well as the M2 marker *Arg1*, Fig. 5A. Macrophages exposed to CNC_{dry} and CNC_{gel} in presence of IL4/IL13 showed reduced expression of M2 markers *Ear11* and *Mrc1*, as well as *Il1b* compared to those polarized without CNC particles (controls), Fig. 5B.

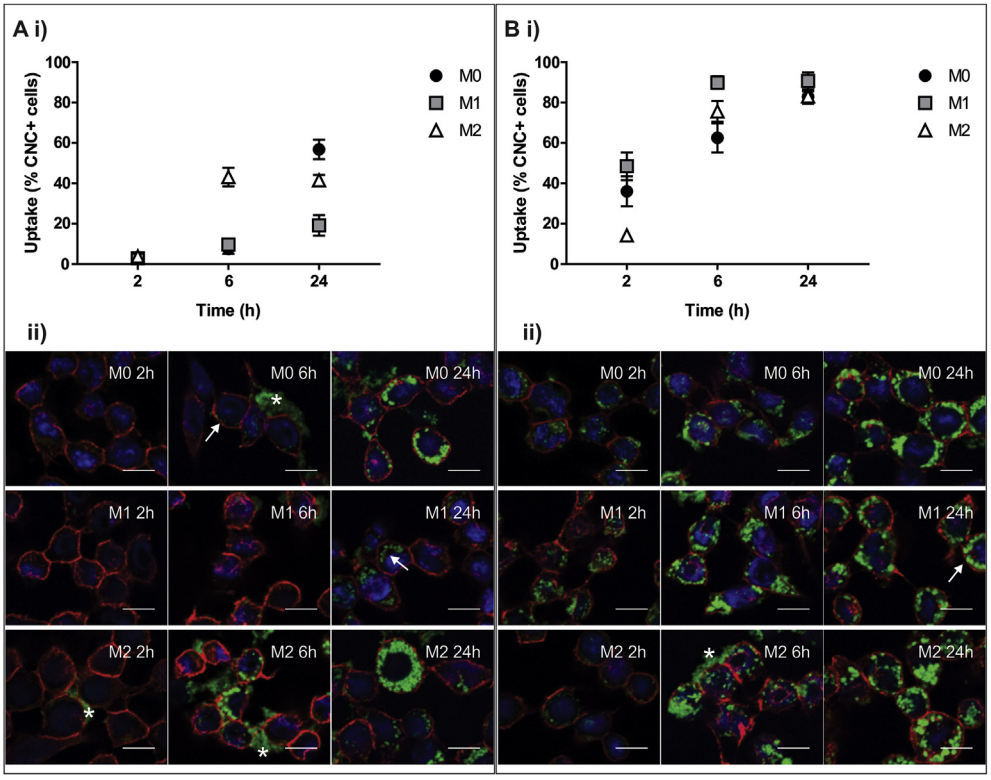

Fig. 2. Cellular uptake of CNC materials. Unpolarized (M0) and polarized (IFNG, M1 and IL4/IL13, M2) macrophages were exposed to 5 μg/cm^2 (A) CNC_{dry} and (B) CNC_{gel} particles for 2, 6, and 24 h. CNC particles were visualized by EXG:CBM staining. (i) Uptake was quantified as percentage of cells with visible vacuoles in the cytoplasm (% CNC + cells). Data represent mean ± SEM. (ii) Representative images of cellular CNC uptake (green). F-actin was stained with phalloidin (red) and nuclei counterstained with DAPI (blue). Images were acquired at 40× magnification. Scale bar, 10 μm. Arrows indicate vacuoles with internalized CNC particles. Asterisks indicate agglomerates of CNC particles.

CNC exposure further altered the secretion of cytokines and chemokines which are involved in the regulation of host defense, inflammation, wound healing, and homeostasis, Fig. 6, Supplementary Table S2. Hierarchical clustering identified defined clusters according to both polarization status and exposure to CNC materials, Fig. 6A. A clear differentiation between control and CNC exposed cells was observed and specific clustering of cells exposed to 45 μg/cm^2 CNC_{gel} in presence of IFNG (M1) indicates that this treatment affected the overall cytokine and chemokine secretion from these cells. Further analysis identified twelve proteins as exclusively regulated following CNC exposure in presence of IFNG (M1) and two proteins following CNC exposure in presence of IL4/IL13 (M2). In addition, the secretion of the six

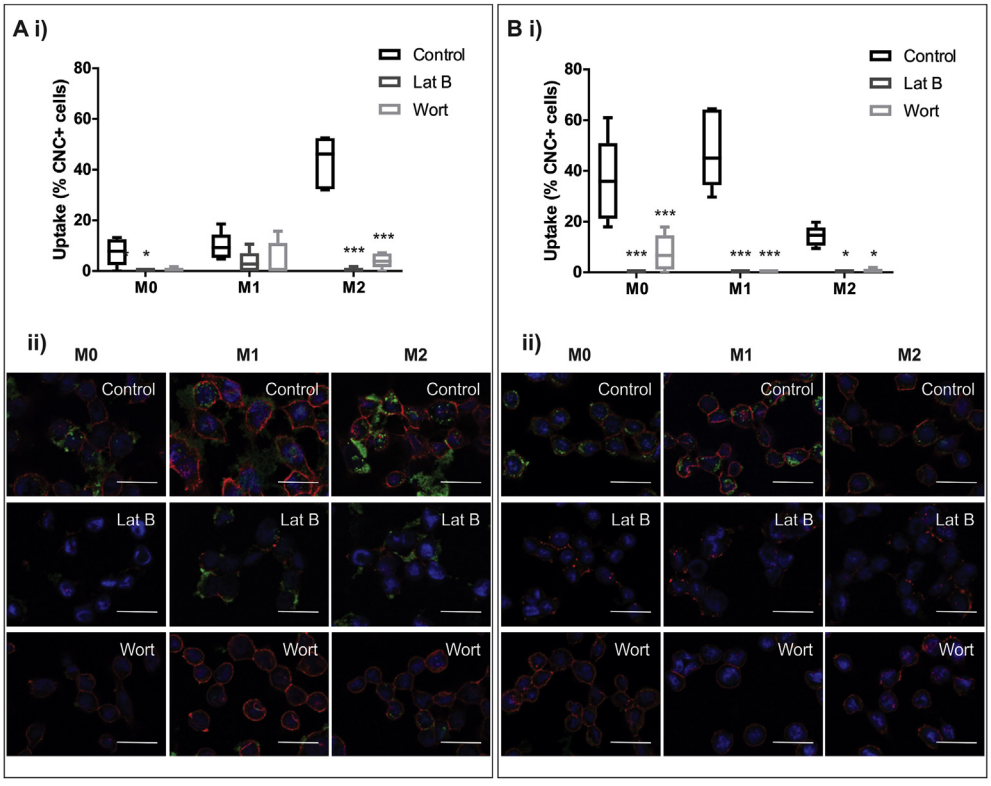

Fig. 3. Mechanisms of cellular uptake of CNC materials. Unpolarized (M0) and polarized (IFNG, M1 and IL4/IL13, M2) macrophages were pretreated with latrunculin B (LatB, 30 min, 2.5 μM) and wortmannin (Wort, 15 min, 300 nM). After pre-incubation the cells were exposed to 5 μg/cm^2 (A) CNC_{dry} for 6 h and (B) CNC_{gel} for 2 h. CNC particles were visualized by EXG:CBM staining. (i) Uptake was quantified as percentage of cells with visible vacuoles in the cytoplasm (% CNC + cells). Data represent median, and 5 and 95 percentiles. (ii) Representative images of cellular CNC uptake (green). F-actin was stained with phalloidin (red) and nuclei counterstained with DAPI (blue). Images were acquired at 40× magnification. Scale bar, 20 μm *p < 0.05, ***p < 0.001 (ANOVA, Dunnett's test).

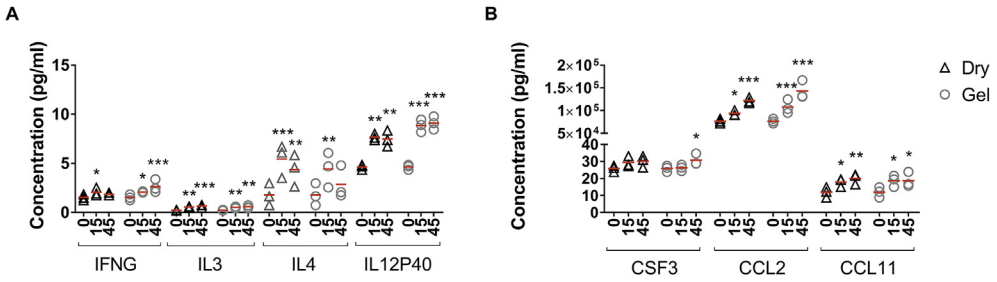

Fig. 4. Effects of CNC exposure on the secretion of cytokines and chemokines from unpolarized macrophages. Secretion of (A) cytokines and (B) chemokines were analyzed using the Luminex MAGPIX® System. Lines represent mean, and open triangles and circles represent individual values, *p < 0.05, **p < 0.01, ***p < 0.001, (n = 3).

proteins IL3, IL9, IL17A, CCL2, CCL4 and CCL5 were regulated following CNC exposure during polarization of both M1 and M2 macrophages, Fig. 6B. Of these only CCL4 was differentially regulated in M1 and M2 cells, Fig. 6C. CNC exposure in presence of IFNG led to increased secretion of the cytokines IL1A, IL1B, IL4, IL6, IL12, IL13 and TNFA, and of the chemokines CSF2 (previously known as GM-CSF), CSF3 and CXCL1 (previously known as GRO1), whereas the secretion of CXCL9 was reduced, Fig. 6D (i)-(iii). This regulation was more prominent following CNC_{gel} exposure. Finally, CNC exposure in presence of IL4/IL13 not only reduced the gene expression of M2 markers *Ear11* and *Mrc1* but also decreased the secretion of the M2 related cytokine IL10 and increased the secretion of the M1 response related CCL11 chemokine, Fig. 6E.

3.6. Effects of CNC exposure on macrophage activity

To study the effects of CNCs on the activity of polarized macrophages, cytokine profiles and effects on bacterial phagocytosis were investigated. Analyses of cytokine secretion from activated macrophages exposed to CNCs showed similar patterns to cells exposed during polarization, however, the effects were more subtle, Supplementary Table S3. Venn diagram analyses identified six proteins; IL3, IL12P40, IL17A, CCL2, CCL5 (previously known as RANTES) and CCL11, with increased secretion levels in both CNC exposed M1 and M2 cells, Fig. 7A. In addition, M1 polarized macrophages had higher secretion of IL1A, IL4, IL5, IL6, IL9, IL12P70 and reduced levels of IL10 and CXCL9 protein following CNC exposure, Fig. 7B and C.

Besides cytokine production, phagocytic bacterial clearance is perhaps the most important activity of alveolar macrophages, which along with mucociliary transport provides an effective, nonspecific pulmonary defense. CNC particles altered macrophage phagocytosis of E. coli bioparticles in a dose dependent manner, Fig. 8. At the lowest concentrations (1.5 μg/cm^2) both CNC_{dry} and CNC_{gel} exposure increased the phagocytic capacity of the cells and also the maturity of phagosomes independent of macrophage phenotype. However, clear differences in phagocytic patterns and the degree of response to CNC exposure were observed between macrophages of different phenotypes. In unpolarized (M0) cells, CNC_{dry} exposure induced phagocytosis at the

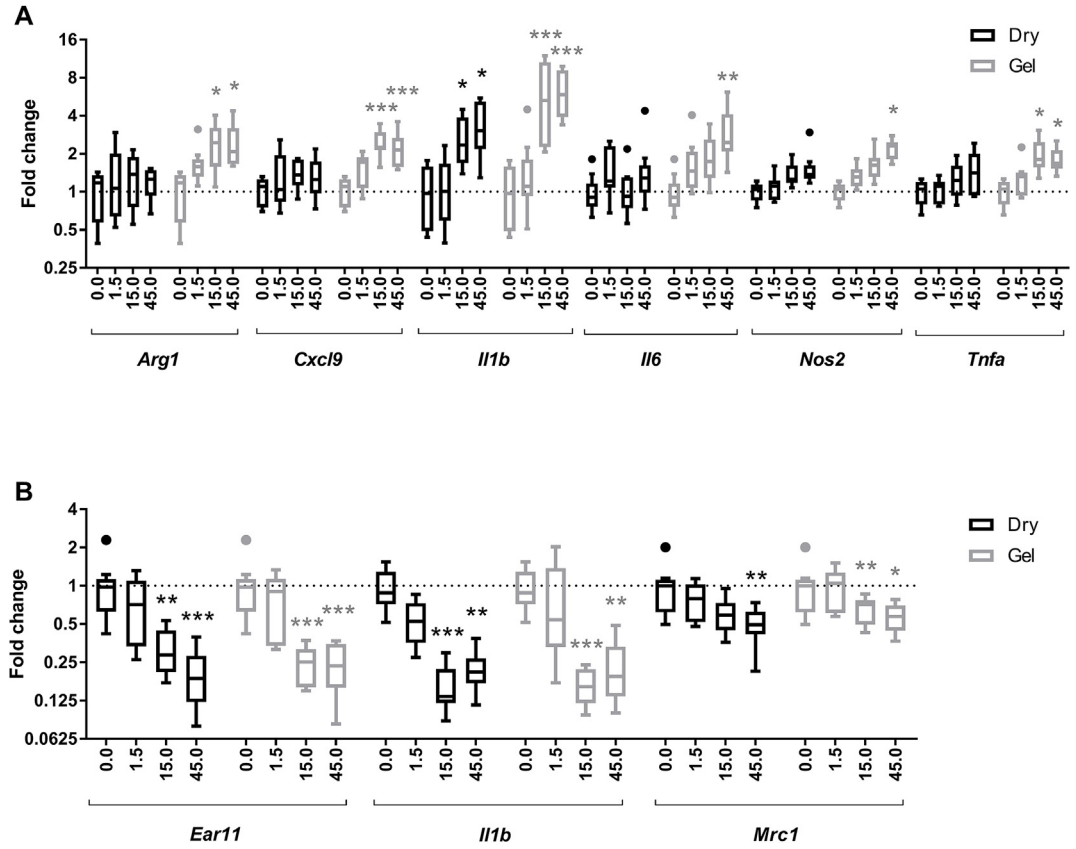

Fig. 5. Effects of CNC exposure on the expression of common macrophage polarization markers. Changes in gene expression were assessed by qPCR following CNC exposure in presence of inducers of polarization (A) IFNG (M1) and (B) IL4/IL13 (M2). Expression was related to unexposed control cells (stimulated with IFNG or IL4/IL13). Boxes indicate median, and 5 and 95 percentiles, (n = 9). *p < 0.05, **p < 0.01, ***p < 0.001.

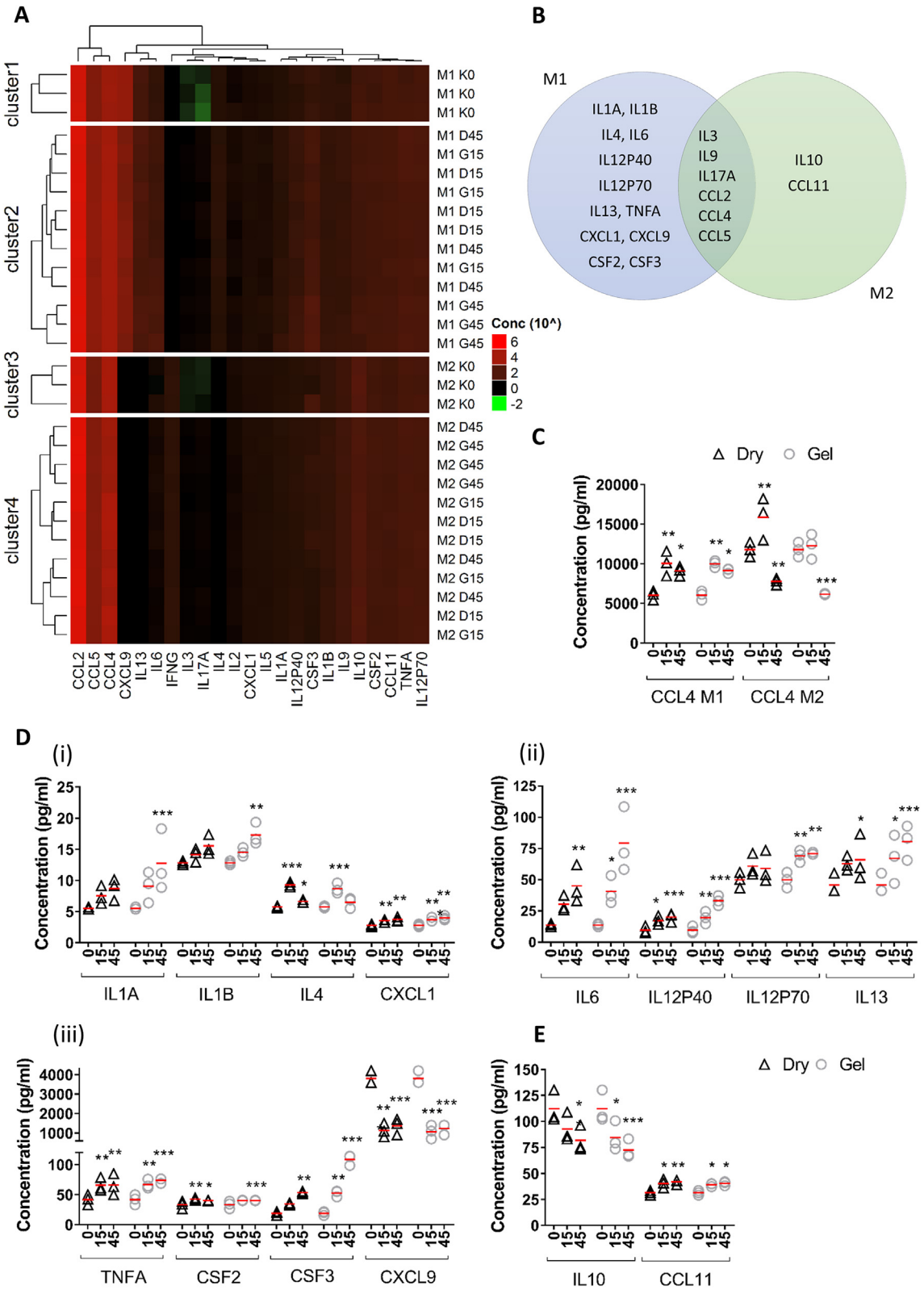

Fig. 6. Effects of CNC exposure on the secretion of cytokines and chemokines in presence of inducers of macrophage polarization. Secretion of cytokines and chemokines was analyzed on the Luminex MAGPIX® System. (A) Regulation of secreted cytokines and chemokines was illustrated by heat map and hierarchical clustering using Euclidean distance. Values represent log 10 scaled concentrations (pg/ml). Concentrations levels are colored green for low intensities and red for high intensities. (B) Venn diagram of proteins regulated following CNC exposure in presence of inducers of macrophage polarization, *i.e.* IFNG (M1) or IL4/IL13 (M2). (C) CCL4 protein levels following CNC exposure in presence of IFNG (M1) and IL4/IL13 (M2). (D) Protein levels following CNC exposure in presence of IFNG (M1). (E) Protein levels following CNC exposure in presence of IL4/IL13 (M2). Unexposed control cells were stimulated with IFNG or IL4/IL13. Lines represent mean, and open triangles and circles represent individual values, *$p < 0.05$, **$p < 0.01$, ***$p < 0.001$, ($n = 3$).

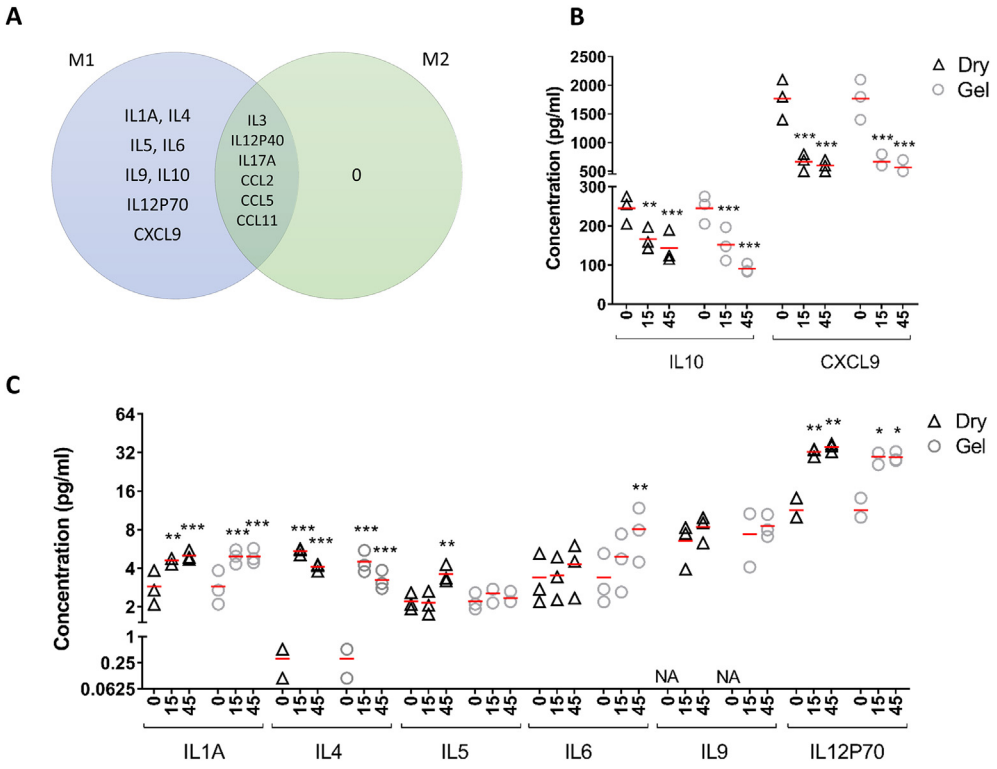

Fig. 7. Effects of CNC exposure on the secretion of cytokines and chemokines from M1 and M2 polarized macrophages. (A) Venn diagram of proteins regulated in M1 and M2 polarized cells. (B) Downregulated and (C) upregulated protein levels following CNC exposure in M1 polarized cells. Lines represent mean, and open triangles and circles represent individual values. NA indicates proteins under detection level, *p < 0.05, **p < 0.01, ***p < 0.001, (n = 3).

lowest concentration (1.5 μg/cm^2) but resulted in reduced phagocytosis at higher concentrations (15 and 45 μg/cm^2). While, M0 cells exposed with 1.5 and 15 μg/cm^2 CNC_{gel} showed increased phagocytosis, exposure to 45 μg/cm^2 CNC_{gel} resulted in reduced overall phagocytic capacity, Fig. 8A. M1 polarized cells showed a generally more rapid initial uptake of bioparticles than M0 and M2 cells. CNC exposure at

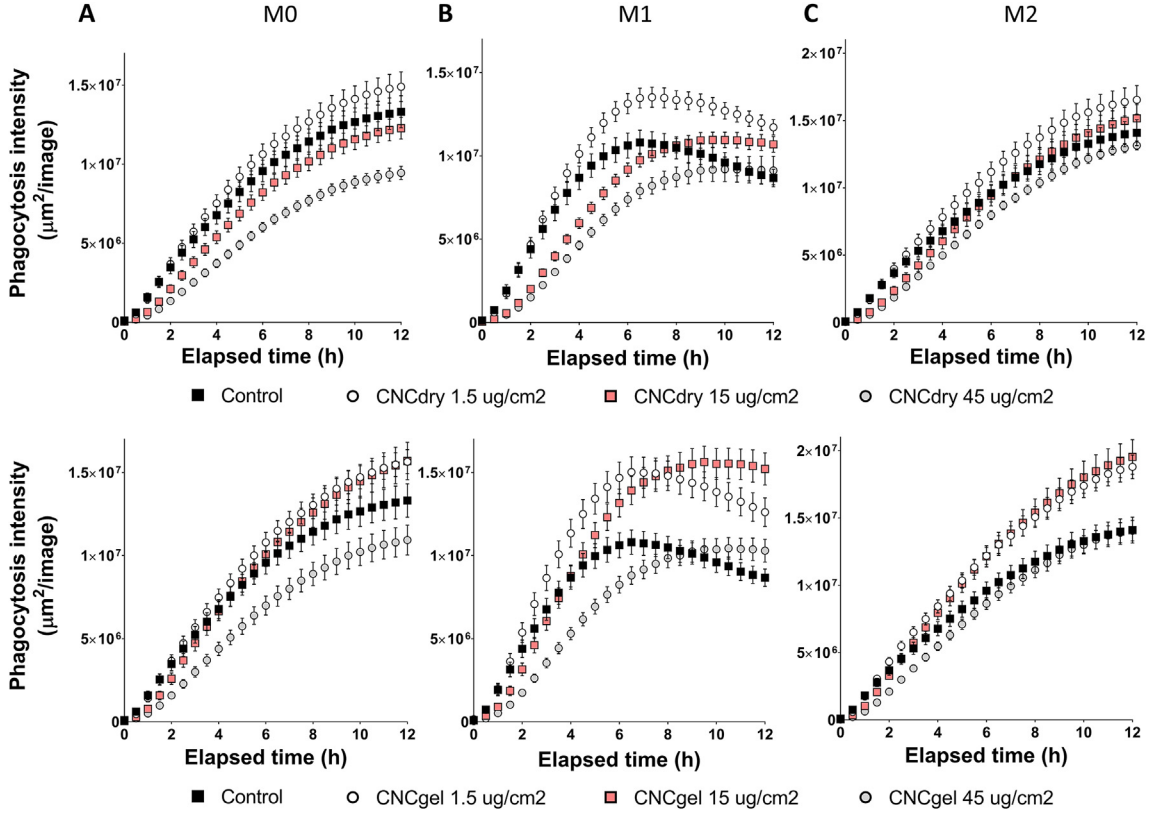

Fig. 8. Effects of CNC exposure on the phagocytic capacity of MH-S macrophages. Phagocytosis of bioparticles was analyzed by live cell imaging using IncuCyte Zoom in unpolarized M0 cells (A), M1 polarized cells (B) and M2 polarized cells (C). Phagocytic capacity is illustrated by Phagocytosis intensity which is a measure of both the number of active phagosomes and their degree of maturation. Data points illustrate mean ± SEM, n = 8.

low concentrations (1.5 and 15 μg/cm^2) increased the total phagocytic capacity of M1 cells. On contrary, high concentrations (45 μg/cm^2) of CNC exposure, reduced the initial uptake of bioparticles in M1 cells leading to a delayed uptake of bioparticles, Fig. 8B. The effects of CNC_{dry} exposure on M2 phagocytosis were very subtle, and CNC_{gel} exposure at 45 μg/cm^2 did not markedly affect M2 cell phagocytosis, Fig. 8C. However, exposure of M2 cells with CNC_{gel} at 1.5 and 15 μg/cm^2 increased both phagosome maturation and the cells overall phagocytic capacity, Fig. 8C.

4. Discussion

To date, data on health effects of exposure to NC in the workplace are largely unavailable, but experimental animal data show induction of acute pulmonary inflammatory responses following exposure to NCs [8–11]. These animals have increased recruitment of inflammatory cells in the lungs, and accumulation of particles in the bronchi, the alveoli, and in the cytoplasm of pulmonary macrophages [8]. Alveolar macrophages, being primarily responsible for alveolar clearance of particulates, are vital in regulating pulmonary inflammatory reactions. Delayed clearance and accumulation of NCs in alveolar macrophages may alter their viability, activation and function.

In this study, effects of pristine CNCs on alveolar macrophage viability and function were investigated. While functionalization may affect the cytotoxic and immunogenic properties of particles, the focus on this study was on pristine particles. Selected particles were required to be well characterized, commercially available and relevant to occupational exposure scenarios. Analysis of hydrodynamic diameter and zeta potential of the selected CNC particles indicated that they were stable in water but had increased occurrence of aggregates and agglomerates in media. Agglomeration of particles may affect their uptake and consequently biological activities. Agglomerates on the cell surfaces were present particularly following exposure to CNC_{dry} particles. Particle size may affect the phagocytic rate of macrophages [24]. Moreover, macrophages phagocyte particles most effectively in the size range 2–3 μm [25]. Thus, it is likely that macrophages could efficiently phagocyte agglomerates of CNC particles in the range of 1–4 μm. Consequently, internalization of CNC materials by alveolar MH-S macrophages was investigated. Previous reports on cellular uptake of NCs indicate that CNCs are taken up by epithelial cells, whereas, CNFs are not [12]. Macrophage uptake of NC has not been studied. Interestingly, macrophage phenotype may affect macrophage uptake of nanoparticles as reported for gold and silica nanoparticles [26–28]. In this study, we observed internalization of CNC_{gel} particles at 2 h post-exposure. CNC_{dry} particles were endocytosed at a much slower rate by the macrophages, and only after 6 h, vacuoles containing CNC were visible in the cytoplasm of the cells. Our study also demonstrated dissimilarities in the kinetics of CNC internalization in differently polarized macrophages. While CNC_{gel} particles were generally more efficiently internalized than CNC_{dry} particles, M2 macrophages have a delayed uptake of CNC_{gel} particles compared with M0 and M1 cells, and M1 cells had a significantly lower uptake of CNC_{dry} particles compared to M0 and M2 macrophages. Mechanisms for CNC endocytosis in macrophages have not been previously investigated. Here we demonstrated that macrophage internalization of CNC_{dry} and CNC_{gel} particles was actin and PI3K dependent. Actin and PI3K dependency is a hallmark of macropinocytosis and phagocytosis [29,30], thus indicating that these mechanisms are main routes of internalization of CNC particles in MH-S cells. Similarly, the structurally related fungal cell wall component chitin is previously reported to be phagocytosed via toll like receptor 2 (TLR2)/chitin binding protein (CBP) binding [31,32].

Furthermore, the biological consequences of CNC uptake on macrophage viability and activation were assessed. CNC exposure at low concentrations (1.5 and 5 μg/cm^2) did not induce cytotoxic responses in alveolar macrophages, and elevated doses only slightly reduced the cell viability. This is in accordance with several previous studies showing that CNC materials have only limited cytotoxic potential in various experimental models [13,33–36] and are only cytotoxic at high concentrations [37–39]. The diverse biological activities of macrophages are mediated by phenotypically distinct subpopulations generated through a process called macrophage polarization [17]. While, several types of particles, including metal nanoparticles (Au, Ag, Co), metal oxide nanoparticles (ZnO, SiO_2, TiO_2), carbon nanotubes (CNT) and even environmental pollutants (*e.g.* diesel exhaust particles, DEP) have been indicated to affect macrophage polarization [18,40–42], data regarding potential effects of NCs are missing. Available data indicate that most nanoparticles induce M1 polarization with few exemptions as reviewed by Miao et al. [18]. Here, we demonstrate that CNC exposure alone was not sufficient in inducing a full polarization phenotype of murine alveolar macrophages. Unpolarized M0 macrophages had a generally low secretion of cytokines and chemokines, but increased IFNG, IL3, IL4, IL12P40, CCL2, CCL11 and CSF3 levels were observed following CNC exposure. The highest induction was observed for IL4, which is a potent inducer of anti-inflammatory signaling and M2 polarization. It should be noted that this study only addressed acute effects of CNC exposure. Interestingly, CNC exposed mice have pronounced acute pro-inflammatory responses following exposure [9–11], which are time-dependently alleviated [11]. Thus, long-term exposures might sustain the immunosuppressive Th2 signaling important in the persistence of inflammatory responses leading to chronic inflammation. This has recently been demonstrated for muti-walled CNT-induced pulmonary inflammation and fibrosis, where an acute initial induction in M1 polarization was followed by a sustained M2 activation in exposed animals [42].

Whilst CNC exposure alone cannot induce a complete polarization, our data suggest that exposure to CNC particles may promote a more prominent M1 phenotype and a pro-inflammatory Th1 response in the presence of other inducers. Indeed, pro-inflammatory cytokines IL3, IL9 and IL17A, and chemokines CCL2, CCL4 and CCL5 were upregulated in cells exposed to particles during both M1 and M2 polarization. These proteins are considered to be common M1 secreted mediators, corresponding to an increased Th1 signaling. In addition, the expression of the common M1 markers *Cxcl9*, *Il1b*, *Il6*, *Tnfa* and *Nos2* was increased following CNC_{gel} exposure in presence of IFNG. Increased levels of M1 secretory products IL1A, IL1B, IL6, IL12, TNFA, CXCL1, CSF2 and CSF3 were also observed. This regulation was more prominent following CNC_{gel} exposure, which is in accordance with observations made on gene expression level and could plausibly indicate that CNC_{gel} particles are more inflammatory potent. Endotoxin, a common contaminant of concern in NC materials, gives increased M1 polarization and pro-inflammatory cytokine production from macrophages. However, the CNC materials used in this study had no endotoxin contamination as shown by LAL analysis. Finally, CNC exposure in presence of IL4/IL13 reduced the gene expression of M2 markers *Ear11* and *Mrc1* as well as the M2 secreted product IL10 and increased the secretion of the M1 response related CCL11 chemokine. These data suggest that CNCs also may affect the immunosuppressive properties of macrophages and be important in the resolution of immune responses. Taken together, the mechanisms of nanoparticle induced macrophage polarization are still unclear, and there are only few available studies. It has been suggested that stimulation of TLR4 and activation of NF-κB by nanoparticles drives macrophages toward a M1 phenotype. However, the diverse contact with macrophages and different internalization mechanisms may contribute to distinct degrees of macrophage polarization [18].

Our findings of CNC-enhanced M1 polarization and increased pro-inflammatory signaling are consistent with data from animal studies indicating that CNC exposure induces an acute immunogenic response in the lungs, characterized by infusion of immune cells and increased secretion of pro-inflammatory cytokines in bronchoalveolar lavage (BAL) of exposed animals [9,10]. Indeed, the reported alterations in cytokine and chemokine levels in BAL from exposed animals are very similar to the responses observed in the current study in murine

macrophages exposed during polarization, with induction of IL1A and TNFA often implicated in the pathogenesis of acute infectious respiratory diseases, and upregulation of IFNG and IL12, suggesting initiation of Th1 immune responses in animals following CNC exposure. A similar increase in pro-inflammatory cytokines was also observed in lung alveolar epithelial cells exposed to CNCs [12,14]. However, studies on CNC derived from cotton showed no alteration in inflammatory markers in exposed human bronchial epithelial cells and 3D cell cultures [35,37]. Furthermore, in line with our findings, a stronger acute inflammatory response was observed in animals exposed to CNC_{gel} compared to those exposed to CNC_{dry} [9]. This suggests that source of CNC and even slight changes in CNC production despite a common source, as well as different functionalization result in changes in morphology which may be critical in inflicting diverse innate inflammatory responses. Although, the pattern of secreted mediators from MH-S macrophages following CNC exposure indicates a predominant M1 mediated profile, it should be noted, that M1 cells polarized in presence of CNC particles also showed induced *Arg1* gene expression and increased secretion of IL4 and IL13 proteins. This may lead to down-regulation of the pro-inflammatory signaling, and is further supported by *in vivo* data showing that CNCs similar to aspirated fibrous particulates, including CNT and NC [16,43,44], have a peak inflammatory response which is gradually time-dependently alleviated [11].

Effects of CNCs on the biological activity of alveolar macrophages in recruitment of other immune cells and in fine-tuning of immune reactions through release of cytokines and chemokines, as well as in the macrophages' phagocytic/microbicidal activity were investigated. Analyses of cytokine secretion from activated macrophages exposed to CNCs showed similar patterns to cells exposed during polarization, however, the effects were more subtle. For both phenotypes increased secretion of IL3, IL12P40, IL17A, CCL2, CCL5 and CCL11 was observed following exposure to CNCs. However, M1 polarized macrophages additionally had higher secretion of IL1A, IL4, IL5, IL6, IL9, IL12P70 and reduced levels of IL10 and CXCL9 protein following CNC exposure. Thus, CNC materials not only induce a more prominent M1 phenotype, but also increase secretion of pro-inflammatory mediators from activated polarized macrophages. Besides cytokine production, phagocytic bacterial clearance is an important function of alveolar macrophages, which along with mucociliary transport provides an effective, non-specific pulmonary defense. It is noteworthy that exposure to various nanoparticles may dramatically affect the phagocytic activity of macrophages [45,46], however, effects of NC have not been previously investigated. This study demonstrates that CNC particles alter macrophage phagocytosis of E. coli bioparticles in a dose-dependent manner. CNC exposure at low concentrations increased the phagocytic rate and overall phagocytic capacity of macrophages, but high doses reduced the phagocytic rate. Moreover, it is evident that CNC_{gel} particles are more potent in inducing these effects. While no data is available on *in vivo* effects of CNC on pulmonary bacterial clearance, decreased phagocytosis and lung bacterial clearance were observed for mice exposed to CNT and Cu nanoparticles [47,48]. Moreover, CNT exposure decreased macrophage phagocytosis of bacteria *in vitro* [48]. In relation to CNTs, decreased phagocytosis of biodurable HARM could be linked to ineffective pulmonary clearance, as the retention time of phagocytosed biodurable nanoparticles is long [49]. HARMs are of specific concern, *i.e.* the fiber pathogenicity paradigm, as these materials are commonly retained in the pleural cavity if translocated from the lung and can cause persistent inflammation, which may lead to irreversible diseases such as fibrosis, formation of mesothelioma and lung cancer [50]. The CNC materials used here had HARM properties and, therefore, similar effects on macrophage phagocytosis are expected. However, surprisingly, our data indicate that CNC exposure at low doses increases phagocytosis. This could possibly be due to priming of macrophage phagocytosis in a paracrine manner following initiation of macrophage activation and cytokine burst. As this study was performed using a single dose it is difficult to say how repeated accumulation of single doses would affect the cells phagocytic activity. It has been suggested that durable nanoparticles may exhaust macrophages capabilities for additional uptake [45]. Thus, evaluation of effects of chronic and high doses are relevant as CNC, being a biodurable HARM could accumulate in macrophages over time, possibly leading to particle overload. Such particle overload can be observed at the highest dose investigated in this study as immunofluorescence imaging of CNC distribution and uptake in macrophages suggest presence of agglomerates on macrophage surfaces. Particle overload might impair the phagocytic uptake of bioparticles. The biological impact of these findings are unclear as the body has an ability to produce more phagocytic cells on demand.

Throughout the study, CNC_{gel} exposure gave greater effects on the analyzed parameters of macrophage activation and function, *i.e.* polarization markers, cytokine levels, and phagocytic activity. The greater effects observed in CNC_{gel} could be due to the higher uptake of CNC_{gel} particles compared to CNC_{dry}, which as a consequence, makes CNC_{gel} more inflammatory potent. The *in vivo* situation is much more complex and a cross-talk between different cell types in the lung and microenvironment would exert an effect on macrophage polarization and activity. Thus, there is a need to further verify the observed effects in a relevant long-term exposure model *in vivo* in order to investigate the functional impact of these findings and to clarify effects of microenvironment signals contributing to the immunological responses to particle exposure.

5. Conclusions

Our findings suggest that CNC exposure alone does not induce macrophage polarization, but in presence of other activators CNC particles cause a more pronounced M1 macrophage phenotype and a depleted M2 phenotype, possibly leading to increased and prolonged pro-inflammatory signaling. Uptake of CNC in macrophages was correlated with an induction of a cytokine burst and alterations in the cells' phagocytic capacity. Altogether, these changes in macrophage phenotype and their biological activities may contribute to acute pulmonary inflammation following CNC exposure and could affect the responses of activated macrophages to infections. Dysregulation of macrophage activation and function is critical in inflammatory responses, and macrophage polarization may thus be a mechanism in the development of chronic pulmonary diseases following occupational exposure to particles. However, these *in vitro* data need to be confirmed in carefully designed *in vivo* experiments.

Funding

This work was supported by the National Institute of Occupational Health, Oslo, Norway [Grant number: 201600262].

Acknowledgments

Prof. Ulla Vogel (National Research Centre for Work Environment, Copenhagen, Denmark) and Dr. Henrik Wolff (Finnish Institute of Occupational Health, Helsinki, Finland) are acknowledged for their kind contribution in cellulose staining and for providing the EXG:CBM protein. We also thank Dr. Tore-Geir Iversen (Oslo University Hospital, Oslo, Norway) for sharing his expertise in endocytosis, Ine Pedersen for her assistance with LAL analysis, and Mina Eriksen and Tiril Schjølberg for excellent technical support.

Appendix A. Supplementary data

Supplementary data related to this article can be found at https://doi.org/10.1016/j.biomaterials.2019.02.025.

Declarations of interest

None.

Data availability

The datasets generated during the current study are available from the corresponding author on reasonable request.

References

[1] J.A. Shatkin, B. Kim, Cellulose nanomaterials: life cycle risk assessment, and environmental health and safety roadmap, Environ. Sci.: Nano 2 (5) (2015) 477–499.
[2] J.B. Rojas, Mauricio, Yhors Ciro, Current trends in the production of cellulose nanoparticles and nanocomposites for biomedical applications, in: M. Poletto (Ed.), Cellulose - Fundamental Aspects and Current Trends, IntechOpen, 2015.
[3] J. Vartiainen, T. Pöhler, K. Sirola, L. Pylkkänen, H. Alenius, J. Hokkinen, U. Tapper, P. Lahtinen, A. Kapanen, K. Putkisto, P. Hiekkataipale, P. Eronen, J. Ruokolainen, A. Laukkanen, Health and environmental safety aspects of friction grinding and spray drying of microfibrillated cellulose, Cellulose 18 (3) (2011) 775–786.
[4] A.B. Stefaniak, M.S. Seehra, N.R. Fix, S.S. Leonard, Lung biodurability and free radical production of cellulose nanomaterials, Inhal. Toxicol. 26 (12) (2014) 733–749.
[5] C. Endes, S. Camarero-Espinosa, S. Mueller, E.J. Foster, A. Petri-Fink, B. Rothen-Rutishauser, C. Weder, M.J.D. Clift, A critical review of the current knowledge regarding the biological impact of nanocellulose, J. Nanobiotechnol. 14 (2016) 78.
[6] J.A. Shatkin, K. Ong, J. Ede, T. Wegner, M. Goergen, Toward Cellulose Nanomaterial Commercialization: Knowledge Gap Analysis for Safety Data Sheets According to the Globally Harmonized System, (2016).
[7] A.B. Seabra, J.S. Bernardes, W.J. Favaro, A.J. Paula, N. Duran, Cellulose nanocrystals as carriers in medicine and their toxicities: a review, Carbohydr. Polym. 181 (2018) 514–527.
[8] J. Catalán, E. Rydman, K. Aimonen, K.-S. Hannukainen, S. Suhonen, E. Vanhala, C. Moreno, V. Meyer, D.d.S. Perez, A. Sneck, U. Forsström, C. Højgaard, M. Willemoes, J.R. Winther, U. Vogel, H. Wolff, H. Alenius, K.M. Savolainen, H. Norppa, Genotoxic and inflammatory effects of nanofibrillated cellulose in murine lungs, Mutagenesis 32 (1) (2017) 23–31.
[9] N. Yanamala, M.T. Farcas, M.K. Hatfield, E.R. Kisin, V.E. Kagan, C.L. Geraci, A.A. Shvedova, In vivo evaluation of the pulmonary toxicity of cellulose nanocrystals: a renewable and sustainable nanomaterial of the future, ACS Sustain. Chem. Eng. 2 (7) (2014) 1691–1698.
[10] A.A. Shvedova, E.R. Kisin, N. Yanamala, M.T. Farcas, A.L. Menas, A. Williams, P.M. Fournier, J.S. Reynolds, D.W. Gutkin, A. Star, R.S. Reiner, S. Halappanavar, V.E. Kagan, Gender differences in murine pulmonary responses elicited by cellulose nanocrystals, Part. Fibre Toxicol. 13 (2016) 28.
[11] E.-J. Park, T.O. Khaliullin, M.R. Shurin, E.R. Kisin, N. Yanamala, B. Fadeel, J. Chang, A.A. Shvedova, Fibrous nanocellulose, crystalline nanocellulose, carbon nanotubes, and crocidolite asbestos elicit disparate immune responses upon pharyngeal aspiration in mice, J. Immunot. 15 (1) (2018) 12–23.
[12] A.L. Menas, N. Yanamala, M.T. Farcas, M. Russo, S. Friend, P.M. Fournier, A. Star, I. Iavicoli, G.V. Shurin, U.B. Vogel, B. Fadeel, D. Beezhold, E.R. Kisin, A.A. Shvedova, Fibrillar vs crystalline nanocellulose pulmonary epithelial cell responses: cytotoxicity or inflammation? Chemosphere 171 (2017) 671–680.
[13] M.J.D. Clift, E.J. Foster, D. Vanhecke, D. Studer, P. Wick, P. Gehr, B. Rothen-Rutishauser, C. Weder, Investigating the interaction of cellulose nanofibers derived from cotton with a sophisticated 3D human lung cell coculture, Biomacromolecules 12 (10) (2011) 3666–3673.
[14] N. Yanamala, E.R. Kisin, A.L. Menas, M.T. Farcas, T.O. Khaliullin, U.B. Vogel, G.V. Shurin, D. Schwegler-Berry, P.M. Fournier, A. Star, A.A. Shvedova, In vitro toxicity evaluation of lignin-(un)coated cellulose based nanomaterials on human A549 and THP-1 cells, Biomacromolecules 17 (11) (2016) 3464–3473.
[15] N. Hadrup, K.B. Knudsen, T. Berthing, H. Wolff, S. Bengtson, C. Kofoed, R. Espersen, C. Højgaard, J.R. Winther, M. Willemoës, I. Wedin, M. Nuopponen, H. Alenius, H. Norppa, H. Wallin, U. Vogel, Pulmonary effects of nanofibrillated celluloses in mice suggest that carboxylation lowers the inflammatory and acute phase responses, Environ. Toxicol. Pharmacol. 66 (2019) 116–125.
[16] M. Ilves, S. Vilske, K. Aimonen, H.K. Lindberg, S. Pesonen, I. Wedin, M. Nuopponen, E. Vanhala, C. Højgaard, J.R. Winther, M. Willemoës, U. Vogel, H. Wolff, H. Norppa, K. Savolainen, H. Alenius, Nanofibrillated Cellulose Causes Acute Pulmonary Inflammation that Subsides within a Month, Nanotoxicology (2018) 1–18.
[17] P.J. Murray, T.A. Wynn, Protective and pathogenic functions of macrophage subsets, Nat. Rev. Immunol. 11 (11) (2011) 723–737.
[18] X. Miao, X. Leng, Q. Zhang, The current state of nanoparticle-induced macrophage polarization and reprogramming Research, Int. J. Mol. Sci. 18 (2) (2017) 336.
[19] M. Kunaver, A. Anžlovar, E. Žagar, The fast and effective isolation of nanocellulose from selected cellulosic feedstocks, Carbohydr. Polym. 148 (2016) 251–258.
[20] S. Chen, I.E. Kammerl, O. Vosyka, T. Baumann, Y. Yu, Y. Wu, M. Irmler, H.S. Overkleeft, J. Beckers, O. Eickelberg, S. Meiners, T. Stoeger, Immunoproteasome dysfunction augments alternative polarization of alveolar macrophages, Cell Death Differ. 23 (6) (2016) 1026–1037.
[21] K.A. Jablonski, S.A. Amici, L.M. Webb, J.D. Ruiz-Rosado, P.G. Popovich, S. Partida-Sanchez, M. Guerau-de-Arellano, Novel markers to delineate murine M1 and M2 macrophages, PLoS One 10 (12) (2015).
[22] D.W. Melton, L.M. McManus, J.A.L. Gelfond, P.K. Shireman, Temporal phenotypic features distinguish polarized macrophages in vitro, Autoimmunity 48 (3) (2015) 161–176.
[23] K.B. Knudsen, C. Kofoed, R. Espersen, C. Højgaard, J.R. Winther, M. Willemoës, I. Wedin, M. Nuopponen, S. Vilske, K. Aimonen, I.E.K. Weydahl, H. Alenius, H. Norppa, H. Wolff, H. Wallin, U. Vogel, Visualization of nanofibrillar cellulose in biological tissues using a biotinylated carbohydrate binding module of β-1,4-glycanase, Chem. Res. Toxicol. 28 (8) (2015) 1627–1635.
[24] M. Zhang, M. Yang, T. Morimoto, N. Tajima, K. Ichiraku, K. Fujita, S. Iijima, M. Yudasaka, T. Okazaki, Size-dependent cell uptake of carbon nanotubes by macrophages: a comparative and quantitative study, Carbon 127 (2018) 93–101.
[25] J.A. Champion, A. Walker, S. Mitragotri, Role of particle size in phagocytosis of polymeric microspheres, Pharm. Res. (N. Y.) 25 (8) (2008) 1815–1821.
[26] H. Herd, K. Bartlett, J. Gustafson, L. McGill, H. Ghandehari, Macrophage silica nanoparticle response is phenotypically dependent, Biomaterials 53 (2015) 574–582.
[27] J. Hoppstädter, M. Seif, A. Dembek, C. Cavelius, H. Huwer, A. Kraegeloh, A.K. Kiemer, M2 polarization enhances silica nanoparticle uptake by macrophages, Front. Pharmacol. 6 (2015) 55.
[28] S.A. MacParland, K.M. Tsoi, B. Ouyang, X.-Z. Ma, J. Manuel, A. Fawaz, M.A. Ostrowski, B.A. Alman, A. Zilman, W.C.W. Chan, I.D. McGilvray, Phenotype determines nanoparticle uptake by human macrophages from liver and blood, ACS Nano 11 (3) (2017) 2428–2443.
[29] M.C. Kerr, R.D. Teasdale, Defining macropinocytosis, Traffic 10 (4) (2009) 364–371.
[30] J.A. Swanson, Shaping cups into phagosomes and macropinosomes, Nat. Rev. Mol. Cell Biol. 9 (8) (2008) 639–649.
[31] Y. Shibata, M. Kogiso, C.-J. Huang, M. Nouri-Shirazi, E. Mizoguchi, C.K. Dorey, Macrophage chitin binding proteins in phagocytosis and M1 activation in response to chitin microparticles (172.27), J. Immunol. 188 (1 Supplement) (2012) 172.27-172.27.
[32] S. Davis, A.M. Cirone, J. Menzie, F. Russell, C.K. Dorey, Y. Shibata, J. Wei, C. Nan, Phagocytosis-mediated M1 activation by chitin but not by chitosan, Am. J. Physiol. Cell Physiol. 315 (1) (2018) C62–C72.
[33] K.B. Male, A.C. Leung, J. Montes, A. Kamen, J.H. Luong, Probing inhibitory effects of nanocrystalline cellulose: inhibition versus surface charge, Nanoscale 4 (4) (2012) 1373–1379.
[34] K.A. Mahmoud, J.A. Mena, K.B. Male, S. Hrapovic, A. Kamen, J.H. Luong, Effect of surface charge on the cellular uptake and cytotoxicity of fluorescent labeled cellulose nanocrystals, ACS Appl. Mater. Interfaces 2 (10) (2010) 2924–2932.
[35] C. Endes, O. Schmid, C. Kinnear, S. Mueller, S. Camarero-Espinosa, D. Vanhecke, E.J. Foster, A. Petri-Fink, B. Rothen-Rutishauser, C. Weder, M.J.D. Clift, An in vitro testing strategy towards mimicking the inhalation of high aspect ratio nanoparticles, Part. Fibre Toxicol. 11 (2014) 40.
[36] S. Dong, A.A. Hirani, K.R. Colacino, Y.W. Lee, M. Roman, Cytotoxicity and cellular uptake of cellulose nanocrystals, Nano LIFE 02 (03) (2012) 1241006.
[37] J. Catalán, M. Ilves, H. Järventaus, K.-S. Hannukainen, E. Kontturi, E. Vanhala, H. Alenius, K.M. Savolainen, H. Norppa, Genotoxic and immunotoxic effects of cellulose nanocrystals in vitro, Environ. Mol. Mutagen. 56 (2) (2015) 171–182.
[38] Z. Hanif, F.R. Ahmed, S.W. Shin, Y.-K. Kim, S.H. Um, Size- and dose-dependent toxicity of cellulose nanocrystals (CNC) on human fibroblasts and colon adenocarcinoma, Colloids Surfaces B Biointerfaces 119 (2014) 162–165.
[39] H. Ni, S.Q. Zeng, J. Wu, X.R. Cheng, T. Luo, W.Y. Wang, W.J. Zeng, Y. Chen, Cellulose nanowhiskers: preparation, characterization and cytotoxicity evaluation, Bio Med. Mater. Eng. 22 (1–3) (2012) 121–127.
[40] M. Jaguin, O. Fardel, V. Lecureur, Exposure to Diesel Exhaust Particle Extracts (DEPe) Impairs Some Polarization Markers and Functions of Human Macrophages through Activation of AhR and Nrf2, PLoS One 10 (2) (2015) e0116560.
[41] N. Labranche, C.E. Khattabi, G. Berkenboom, S. Pochet, Effects of diesel exhaust particles on macrophage polarization, Hum. Exp. Toxicol. 36 (4) (2016) 412–420.
[42] J. Dong, Q. Ma, Macrophage polarization and activation at the interface of multi-walled carbon nanotube-induced pulmonary inflammation and fibrosis, Nanotoxicology 12 (2) (2018) 153–168.
[43] R.R. Mercer, J. Scabilloni, L. Wang, E. Kisin, A.R. Murray, D. Schwegler-Berry, A.A. Shvedova, V. Castranova, Alteration of deposition pattern and pulmonary response as a result of improved dispersion of aspirated single-walled carbon nanotubes in a mouse model, Am. J. Physiol. Lung Cell Mol. Physiol. 294 (1) (2008) L87–L97.
[44] A.A. Shvedova, E. Kisin, A.R. Murray, V.J. Johnson, O. Gorelik, S. Arepalli, A.F. Hubbs, R.R. Mercer, P. Keohavong, N. Sussman, J. Jin, J. Yin, S. Stone, B.T. Chen, G. Deye, A. Maynard, V. Castranova, P.A. Baron, V.E. Kagan, Inhalation vs. aspiration of single-walled carbon nanotubes in C57BL/6 mice: inflammation, fibrosis, oxidative stress, and mutagenesis, Am. J. Physiol. Lung Cell Mol. Physiol. 295 (4) (2008) L552–L565.
[45] S. Bancos, D.L. Stevens, K.M. Tyner, Effect of silica and gold nanoparticles on macrophage proliferation, activation markers, cytokine production, and phagocytosis in vitro, Int. J. Nanomed. 10 (2015) 183–206.
[46] D. Akilbekova, R. Philiph, A. Graham, K.M. Bratlie, Macrophage reprogramming: influence of latex beads with various functional groups on macrophage phenotype and phagocytic uptake in vitro, J. Biomed. Mater. Res. 103 (1) (2015) 262–268.
[47] J.S. Kim, A. Adamcakova-Dodd, P.T. O'Shaughnessy, V.H. Grassian, P.S. Thorne, Effects of copper nanoparticle exposure on host defense in a murine pulmonary infection model, Part. Fibre Toxicol. 8 (1) (2011) 29.
[48] A.A. Shvedova, J.P. Fabisiak, E.R. Kisin, A.R. Murray, J.R. Roberts, Y.Y. Tyurina,

J.M. Antonini, W.H. Feng, C. Kommineni, J. Reynolds, A. Barchowsky, V. Castranova, V.E. Kagan, Sequential exposure to carbon nanotubes and bacteria enhances pulmonary inflammation and infectivity, Am. J. Respir. Cell Mol. Biol. 38 (5) (2008) 579–590.

[49] M. Geiser, W.G. Kreyling, Deposition and biokinetics of inhaled nanoparticles, Part. Fibre Toxicol. 7 (2010) 2.

[50] K. Donaldson, F.A. Murphy, R. Duffin, C.A. Poland, Asbestos, carbon nanotubes and the pleural mesothelium: a review of the hypothesis regarding the role of long fibre retention in the parietal pleura, inflammation and mesothelioma, Part. Fibre Toxicol. 7 (1) (2010) 5.